

Supporting Information

A Thermoplastic PMMA@W₁₈O₄₆ Nanocomposite for UVC Optical Detection

Lidia Mezzina^{1,2}, Angelo Nicosia¹, Antonino Mazzaglia³, Maria Pia Casaletto⁴, Yanqiu Zhu⁵ and Placido G. Mineo^{1,6}*

¹Department of Chemical Sciences, University of Catania, Viale A. Doria 6, 95125 Catania, Italy

²Ann and H.J. Smead Department of Aerospace Engineering Sciences, 3775 Discovery Drive, University of Colorado Boulder, Boulder, CO 80303, USA

³National Council of Research, Institute of Nanostructured Materials (CNR-ISMN), URT of Messina c/o Department of Chemical, Biological, Pharmaceutical and Environmental Sciences, University of Messina, Viale F. Stagno d'Alcontres 31, 98166 Messina, Italy

⁴National Council of Research, Institute of Nanostructured Materials (CNR-ISMN), Via U. La Malfa 153, 90146 Palermo, Italy

⁵College of Engineering, Mathematics and Physical Sciences, University of Exeter, Exeter EX4 4QF, UK

⁶Institute for Chemical and Physical Processes (CNR-IPCF), Viale F. Stagno d'Alcontres 37, I-98158, Messina, Italy

Content

- Emission spectrum of the UVC lamp
- FT-IR spectra of PMMA and PMMA@W₁₈O₄₉
- Structural and electronic characterization of W₁₈O₄₉ nanorods

Emission spectrum of the UVC lamp

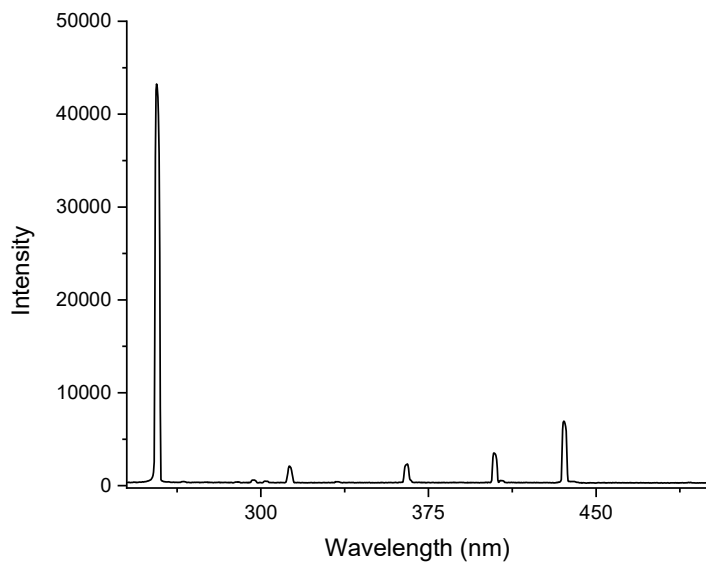


Figure S1. Emission spectrum of the UVC lamp

FT-IR spectra of PMMA and PMMA@W₁₈O₄₉

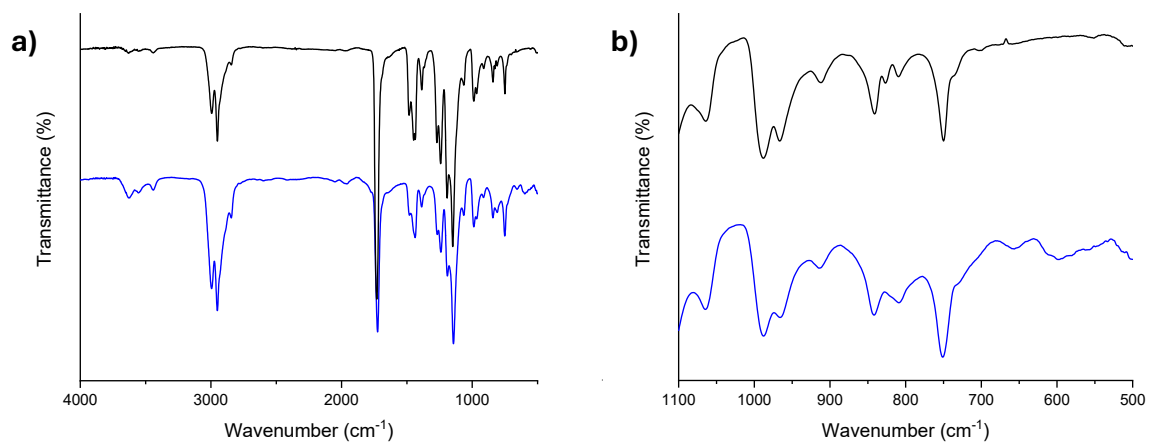


Figure S2. a) FT-IR spectra of PMMA (black line) and PMMA@W₁₈O₄₉ (blue line) and related zoom (b) of the range 1100-500 cm⁻¹.

Structural and electronic characterization of $W_{18}O_{49}$ nanorods.

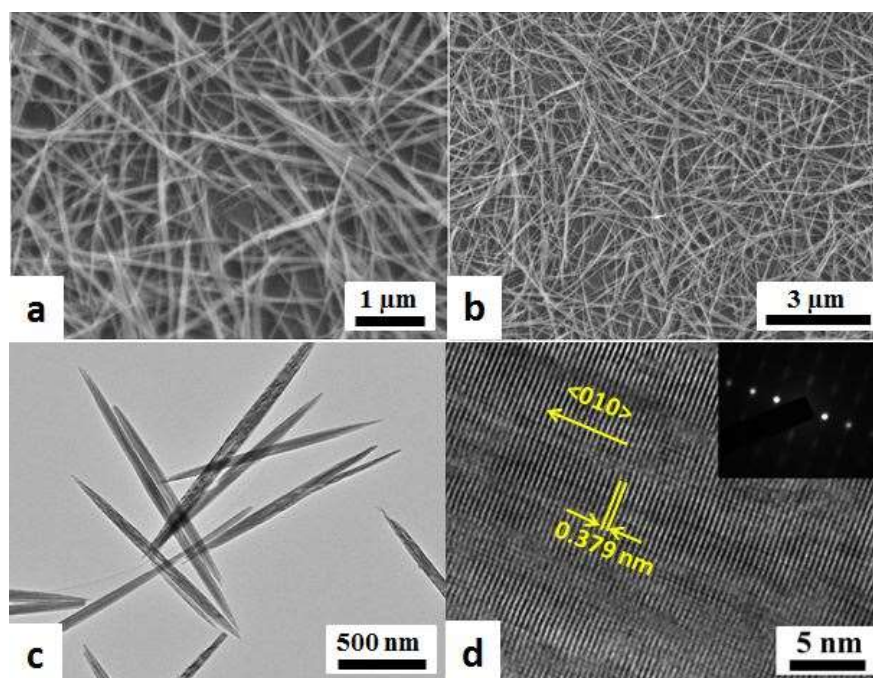


Figure S3. SEM images of the pristine $W_{18}O_{49}$ nanowire bundles at high and low magnifications, (a and b, respectively). Low and high magnification TEM images of the $W_{18}O_{49}$ nanowire bundles, (c and d, respectively). Inset in (d) is the corresponding SAED pattern.

The SEM images in Figure S3a and b show that each bundle is about 50 nm in diameter and up to 3 μm in length. TEM analysis confirmed that these as-prepared $W_{18}O_{49}$ nanowires consisted of ultrathin nanowires of only *ca.* 2-5 nm in diameter and up to 2 μm in length, which were self-assembled into larger bundles. Further, SAED pattern and corresponding HRTEM lattice images (Figure S3c and d) showed that these nanowires are all single crystalline, with the same growth axis (i.e. the nanowire axis) along the $\langle 010 \rangle$ direction, perpendicular to the parental (010) which has a spacing of 0.379 nm. This is a typical character of the bundled 1-D nanostructured materials.

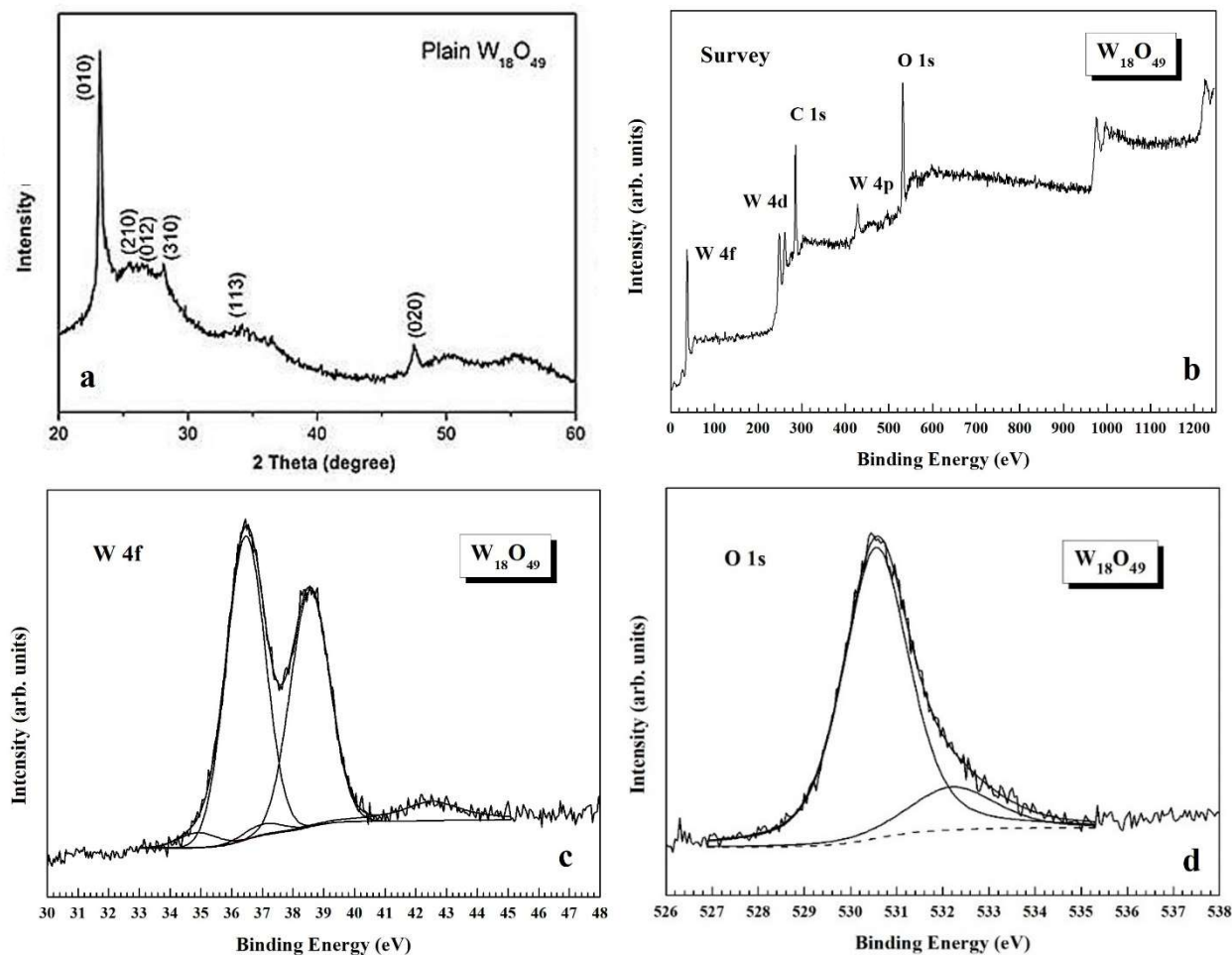


Figure S4. (a) XRD pattern, (b) XPS survey spectra, (c) and (d) XPS curve-fitting of the high-resolution W 4f and O 1s photoelectron signals of the bundled $W_{18}O_{49}$ nanowires, respectively.

The XRD patterns (Figure S4a) of the synthesised WO_x match well with JCPDS No: 01-073-2177, confirming the dominant base crystalline feature of the $W_{18}O_{49}$ monoclinic phase, with lattice constants of $a = 0.1832$, $b = 0.379$, $c = 1.404$ nm, and $\beta = 115.03^\circ$. Two main diffraction peaks at 2θ at about 23.2° and 47.5° can be assigned to the (010) and (020), respectively (Figure S4a). The strongest intensity of the (010) plane is indicative of that the nanowires are preferably grown along the $\langle 010 \rangle$ direction, and thus very weak intensities of other planes in the profiles, such as (210), (012), (310) and (113), which is a typical feature of the 1-dimensional nanowires. The d value of plane (010) derived from the XRD pattern is 0.379 nm, which matches well with the d value from the SAED pattern of $W_{18}O_{49}$ nanowire bundles (Figure S3).

The XPS survey spectrum of the $W_{18}O_{49}$ nanowires is shown in Figure S4b. The atomic concentration percentages of O and W are 74.4 and 25.6, respectively. The results of the curve-

fitting of the W 4f and O 1s signals of the W₁₈O₄₉ nanorods are shown in Figure S4c and d, respectively. The W 4f core level spectrum of the W₁₈O₄₉ sample can be deconvoluted into two doublets of W 4f_{7/2} and W 4f_{5/2} components. The main doublet consists of W 4f_{7/2} and W 4f_{5/2} components located at BE = 36.4 eV and 38.6 eV, respectively, and assigned to the W⁶⁺ oxidation state, as in WO₃. The W 4f_{7/2} and W 4f_{5/2} components of the second doublet at BE = 34.9 eV and 37.0 eV, respectively, are attributed to the presence of the W⁵⁺ oxidation state. The peak located at ~ BE = 42.5 eV corresponds to a loss feature.

In the curve-fitting of the O 1s spectrum (Figure S4d) two main components were observed, located at BE = 530.8 eV and 532.4 eV. The peak at lower binding energy corresponds to the oxygen O²⁻ species in the lattice of oxide. The higher binding energy peak can be attributed to O²⁻, O⁻, and OH⁻ species in the oxygen-deficient regions.¹⁻³

REFERENCES

(1) Thummavichai, K.; Thi, L. A.; Pung, S.-Y.; Ola, O.; Hussain, M. Z.; Chen, Y.; Xu, F.; Chen, W.; Wang, N.; Zhu, Y. Sodium Tungsten Oxide Bronze Nanowires Bundles in Adsorption of Methylene Blue Dye under UV and Visible Light Exposure. *Energies* 2021, 14 (5). DOI: 10.3390/en14051322.

(2) Thummavichai, K.; Wang, N.; Cheong Lem, L.; Phillips, M.; Ton-That, C.; Chang, H.; Hu, C.; Xu, F.; Xia, Y.; Zhu, Y. Lanthanide-doped W₁₈O₄₉ nanowires: Synthesis, structure and optical properties. *Materials Letters* 2018, 214, 232-235. DOI: 10.1016/j.matlet.2017.12.022.

(3) Wagner, C.; Naumkin, A.; Kraut-Vass, A.; Allison, J.; Powell, C.; Rumble Jr, J. NIST standard reference database 20, Version 3.4 (Web version). National Institute of Standards and Technology: Gaithersburg, MD 2003, 20899.